Effects of Re on crystallographic and magnetic properties of Gd(Fe,Re)$_{12}$

W. G. Chu,[1] G. H. Rao,[1] H. F. Yang,[1] G. Y. Liu,[1] and J. K. Liang[1,2]

[1]*Institute of Physics and Center for Condensed Matter Physics, Chinese Academy of Sciences, Beijing 100080, People's Republic of China*

[2]*International Center for Materials Physics, Chinese Academy of Sciences, Shenyang 110015, People's Republic of China*

In this paper ternary compounds GdFe$_{12-x}$Re$_x$ with x ranging from 1.0 to 2.4 have been synthesized and investigated by means of x-ray powder diffraction (XRD) and magnetic measurements. The compounds crystallize in the tetragonal ThMn$_{12}$ structure with space group $I4/mmm$. Rietveld refinement of the XRD data revealed the preferential occupation of Re over the $8i$ site, which is essentially associated with the atomic size effect. The lattice parameter a and the cell volume V increase with Re content while c holds almost constant. The Curie temperature and saturation moment exhibit linear decreases with increasing Re content. Within the framework of the spin-fluctuation theory the reduction of the Curie temperature is determined mainly by the reduction of the average Fe moment caused primarily by the substitutional disorder of Re for Fe located at the $8i$ site. It was found that the magnetocrystalline anisotropy of GdFe$_{12-x}$Re$_x$ changes from uniaxial to probably canted to planar with increasing x, which could be attributed to the competition between ferromagnetic and antiferromagnetic exchange interactions caused by the variation of the nearest-neighbor distance between Fe atoms and the disorder occupation of Re over the $8i$ site.

　　　　PACS number(s): 75.50.Cc, 75.30.Cr, 75.30.Gw, 61.66.Dk

I. INTRODUCTION

Since the discovery of the ternary Nd$_2$Fe$_{14}$B intermetallic compound with high permanent magnetic performance, a worldwide exploration of novel ternary systems of the type R-G-U (R=rare earth, G=transition metal, U=transition metal or metalloids) for permanent magnet purpose has been carried out intensively.[1–5] Among these systems, the R(Fe,U)$_{12}$ compounds have attracted considerable attention owing to their relatively high Curie temperatures and saturation magnetization as well as large uniaxial magnetocrystalline anisotropy at room temperature.

The R(Fe,U)$_{12}$ compounds crystallize in the tetragonal ThMn$_{12}$ structure with space group $I4/mmm$. In this structure the R atoms occupy the single $2a$ crystallographic site and the Fe atoms fully occupy the $8f$ and $8j$ sites, while the $8i$ site is populated by a mixture of Fe and U atoms (U=Ti, V, Nb, Mo, etc.).[6–10] An exception occurs when U=Si. In RFe$_{10}$Si$_2$ the Si atoms share the $8f$ and $8j$ positions with the Fe atoms.[11] These observations can be qualitatively understood by taking into account the atomic size and/or enthalpy effects.[12] It has been established that the structure-stabilizing element U not only plays a key role in the formation of the R(Fe,U)$_{12}$ structure, but also has a strong influence on the magnetic properties. Generally, irrespective of the rare earth involved, the Curie temperatures, Fe moment and magnetocrystalline anisotropy of the R(Fe,U)$_{12}$ compounds all decrease with increasing U content.[13–18] For many R(Fe,U)$_{12}$ compounds various spin reorientations are expected to occur, since the anisotropy contributions from the Fe sublattice and the R sublattice are of comparable magnitudes but opposite in sign. Although a change of the magnetocrystalline anisotropy behavior from uniaxial to planar in the NdFe$_{12-x}$Mo$_x$ and YFe$_{12-x}$Mo$_x$N$_y$ has been observed with increasing Mo content,[19,20] few investigations have fo-

cused on the effect of U on changing the magnetocrystalline anisotropy type of the Fe sublattice in the R(Fe,U)$_{12}$ compounds. In this contribution, we select Re as the structure-stabilizing element for the following reasons. A large scattering contrast between Re and Fe allows the preferential occupancies of Re over different crystallographic positions in the Gd(Fe,Re)$_{12}$ structure to be accurately determined by Rietveld refinement of x-ray powder-diffraction (XRD) data. On the other hand, for most stabilizing elements U=Ti, V, Cr, Mn, Mo, W, etc., their atomic radii are larger than that of Fe and the enthalpy of solution of U in R are positive; both effects favor a preferential occupancy of U over the $8i$ site.[12] In contrast, the atomic radius of Re is much larger than that of Fe and the enthalpy of solution of Re in Gd is negative, which may provide an opportunity to investigate the competing effects of atomic size and enthalpy on the formation of the Gd(Fe,Re)$_{12}$ compound and on the preferential occupation of Re. Since the Gd sublattice has no contribution to the (crystalline electric field) CEF-induced anisotropy of the Gd(Fe,Re)$_{12}$ compound, it is convenient to study the influence of Re on the contribution of the Fe sublattice to the anisotropy.

The present paper is organized as follows. Section II describes experimental details. Section III presents the experimental results. Section IV is concerned with discussion of crystallographic and magnetic properties of the Gd(Fe,Re)$_{12}$ compound. A summary and a general conclusion are given in Sec. V.

II. EXPERIMENTAL DETAILS

Samples of GdFe$_{12-x}$Re$_x$ with x=0.6, 0.8, 1.0, 1.2, 1.4, 1.8, 2.0, 2.2, 2.4, 2.6, and 2.8 were prepared by arc melting of stoichiometric amounts of constituting elements Gd, Fe, and Re with purity better than 99.9% under high-purity argon atmosphere. Appropriate excess amounts of Gd were added

to compensate the weight loss during arc melting and subsequent heat treatment. The alloy ingots were melted several times to ensure homogeneity. Alloys thus obtained were sealed in an evacuated quartz tube and homogenized at 1373 K for 10 days. To avoid possible phase transformation during cooling, the quartz tube was quenched into water.

XRD experiments were performed by using a Rigaku D/max 2500 diffractometer with Cu $K\alpha$ radiation (40 kV $\times$300 mA) and a graphite monochromator. A step-scan mode was adopted with a sampling time of 1 s and a step width of $2\theta = 0.02°$. Curves of magnetization vs temperature (M-T) of the samples were measured by using a vibrating sample magnetometer in a field of 0.05 T, from which the Curie temperatures can be derived by extrapolating M^2 to zero. Field dependencies of the magnetization (M-H) of the free fine-powder and magnetically aligned samples at 5 K were measured by using a superconducting quantum interference device magnetometer. Saturation moments at 5 K were obtained from the M-H curves of the free fine-powder samples according to the law of approach to saturation. The easy-magnetization direction (EMD) of Gd(Fe,Re)$_{12}$ at room temperature was determined by XRD experiments on the
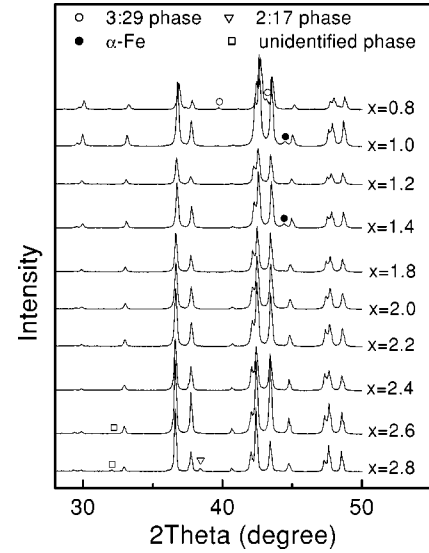

FIG. 1. XRD patterns of GdFe$_{12-x}$Re$_x$ with various x values.

TABLE I. Rietveld refinement results for the GdFe$_{11}$Re and GdFe$_{10.8}$Re$_{1.2}$ compounds with $I4/mmm$, occupancy of Re atom, distances and average distances of sites to neighboring Fe.

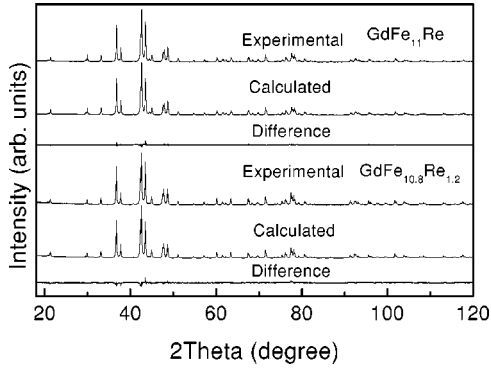|	Atoms	Sites	x	y	z	Distance and average distances of sites to neighboring Fe (Å)		Re (%) occupancy	Number of nearest neighbors
GdFe$_{11}$Re	Gd	2a	0.0	0.0	0.0		3.130		20Fe
	Fe/Re	8i	0.3579(1)	0.0	0.0	8i×1 2.4253	2.706	11.77	13Fe+1Gd
						8i×4 2.9336			
						8j×2 2.6484			
						8j×2 2.6399			
						8f×4 2.6107			
	Fe	8j	0.2759(1)	0.5	0.0	8i×2 2.6484	2.580		10Fe+2Gd
						8i×2 2.6399			
						8j×2 2.7046			
						8f×4 2.4529			
	Fe	8f	0.25	0.25	0.25	8i×4 2.6107	2.501		10Fe+2Gd
						8j×4 2.4529			
						8f×2 2.3802			
						$a=b=8.5339(1)$, $c=4.7603(1)$ Å, $V=346.1(1)$ Å^3, $R_p=5.54\%$, $R_{wp}=7.27\%$, $R_{exp}=4.39\%$			
GdFe$_{10.8}$Re$_{1.2}$	Gd	2a	0.0	0.0	0.0		3.139		20Fe
	Fe/Re	8i	0.3591(1)	0.0	0.0	8i×1 2.4070	2.700	14.69	13Fe+1Gd
						8i×4 2.9256			
						8j×2 2.6256			
						8j×2 2.6343			
						8f×4 2.6160			
	Fe	8j	0.2732(2)	0.5	0.0	8i×2 2.6256	2.581		10Fe+2Gd
						8i×2 2.6343			
						8j×2 2.7396			
						8f×4 2.4525			
	Fe	8f	0.25	0.25	0.25	8i×4 2.6161	2.503		10Fe+2Gd
						8j×4 2.4525			
						8f×2 2.3796			
						$a=b=8.5415(1)$, $c=4.7592(1)$ Å, $V=347.2(1)$ Å^3, $R_p=8.19\%$, $R_{wp}=10.43\%$, $R_{exp}=6.07\%$			

FIG. 2. Experimental XRD patterns and calculated XRD profiles of $GdFe_{11}Re$ and $GdFe_{10.8}Re_{1.2}$, and the differences between the experimental and calculated data.

FIG. 3. Re content dependences of the lattice parameters a, c and the unit-cell volume V.

magnetically aligned samples. Magnetocrystalline anisotropy field at 5 K was derived from the $\Delta M (\Delta M = M_\parallel - M_\perp)$ vs H curves by extrapolating ΔM to zero, where $M_\parallel$ and $M_\perp$ are magnetizations of the free fine-powder and magnetically aligned samples with an applied field perpendicular to the aligned direction, respectively.

III. EXPERIMENTAL RESULTS

A. Crystallographic properties

Phase purity of the samples of $GdFe_{12-x}Re_x$ was examined by XRD and thermomagnetic analysis. Samples with $x = 1.0 – 2.4$ are of almost single phase crystallizing in the tetragonal $ThMn_{12}$ structure except for a very small amount of α-Fe as impurity for $x = 1.0$ and 1.4. The 3:29 phase, an unidentified phase, and the 2:17 phase and the unidentified phase appeared in the samples with $x = 0.8$, 2.6, and 2.8, respectively, as illustrated in Fig. 1.

We adopted the tetragonal $ThMn_{12}$ structure with space group $I4/mmm$ as the initial structure to refine the XRD data of $GdFe_{12-x}Re_x$ using the DWB94-11 program.[21,22] Owing to the large difference in scattering factor between Re and Fe, the preferential occupancy of Re over different positions in $GdFe_{12-x}Re_x$ can be accurately determined by Rietveld refinement of the XRD data. Upon performing the Rietveld refinement, we purposely placed Re on all possible crystal-
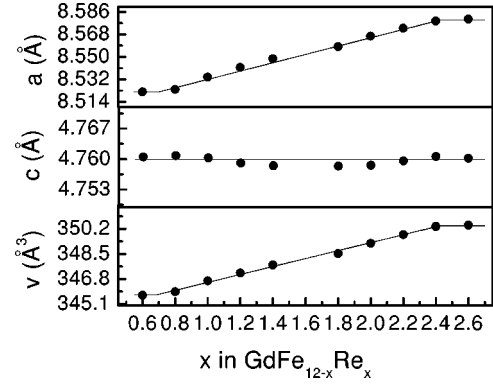
lographic sites and then refined the occupancies over different positions as free parameters. The refinement results revealed that the $8i$ site is populated by a mixture of Re and Fe atoms, and the $8j$ and $8f$ sites are fully occupied by Fe atoms for $GdFe_{12-x}Re_x$ with x ranging from 1.0 to 2.4. The refinement results of the XRD data on $GdFe_{11}Re$ and $GdFe_{10.8}Re_{1.2}$ are shown in Table I and Fig. 2. Based on the Rietveld refinement results regarding the occupancies of Re over the $8i$ site in the $GdFe_{12-x}Re_x$ structure, the formulas of $GdFe_{11.06}Re_{0.94}$ and $GdFe_{10.82}Re_{1.18}$ were derived, for the samples $GdFe_{11}Re$ and $GdFe_{10.8}Re_{1.2}$, respectively, which agree well with the nominal compositions. Chemical analysis of the sample with $x = 1.2$ by an inductively coupled plasma atomic emission spectroscopy (ICP-AES, TJA Co.) gave a stoichiometry of $GdFe_{10.8(1)}Re_{1.23(3)}$.

The lattice parameters a and c and the cell volume V of $GdFe_{12-x}Re_x$ are presented in Table II. Figure 3 shows the dependences of the lattice parameters a and c as well as the volume V of unit cell on x in $GdFe_{12-x}Re_x$. In the single-phase regime the lattice parameter a and the unit-cell volume V increase with increasing x at rates of 0.033 $Å^3$ and 2.66 $Å^3$ per Re atom, respectively, while c holds nearly constant. As has been pointed out above, the Re atoms exclusively occupy the $8i$ site lying in the ab plane. Since the atomic size of Re is larger than that of Fe, the replacement of Fe by Re primarily leads to the increase of a but hardly exerts an influence on c. Assuming that Re and Fe atoms

TABLE II. Structural and magnetic properties of $GdFe_{12-x}Re_x$.

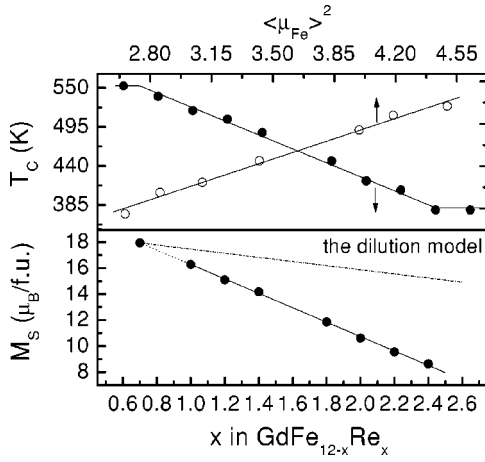| x	a (Å)	c (Å)	V(Å^3)	T_C (K)	$M_S(\mu_B$/f.u.)	H_A (T)	EMD
0.6	8.522	4.760	345.69	553			
0.8	8.524	4.761	345.93	538			
1.0	8.534	4.760	346.67	518	16.3	5.64	c axis
1.2	8.542	4.759	347.20	506	15.1	4.05	c axis
1.4	8.549	4.759	347.75	487	14.2	2.89	c axis
1.8	8.558	4.758	348.52	447	11.9	1.26	c axis
2.0	8.567	4.759	349.22	419	10.6	1.00	c axis
2.2	8.573	4.760	349.81	406	9.6	−0.98	Canted
2.4	8.579	4.760	350.37	378	8.6	−1.59	Planar
2.6	8.580	4.760	350.44	378			

FIG. 4. Dependences of the Curie temperature T_C and the saturation moment M_S on Re concentration, and dependence of T_C on the square of the average Fe moment $\langle \mu_{Fe} \rangle^2$.

both behave as rigid spheres, one can derive an atomic volume difference of 2.43 Å^3, close to 2.66 Å^3, the cell volume increase caused by the substitution of Re for one Fe atom.

Based on the result shown in Fig. 3, the homogeneous regime of GdFe$_{12-x}$Re$_x$ should be $x = 0.7-2.4$, although most single-phase samples were synthesized only for $x = 1.0-2.4$ under present experimental conditions. This statement will be further corroborated by subsequent determination of the Curie temperatures.

B. Magnetic properties

1. The Curie temperatures and saturation moments

The Curie temperatures T_C of GdFe$_{12-x}$Re$_x$ were obtained by plotting the M^2-T curves and extrapolating M^2 to zero. Saturation moments M_S at 5 K are derived from the M-$1/H$ curves of the free fine-powder samples by extrapolating $1/H$ to zero. The Curie temperatures and saturation magnetization are given in Table II. Dependences of T_C and M_S on the Re concentration are illustrated in Fig. 4. It is worthwhile to mention that from the Rietveld refinement results the content of α-Fe as impurity could be estimated to be about 2.7 wt. % and 4.2 wt. % in the samples with $x = 1.0$ and 1.4, respectively. Such a low level of α-Fe as impurity should have no significant effect on the composition dependence of T_C and M_S.

In the intermetallic compounds based on magnetic rare earth (R) and transition metals (G), it is found as a rule that $4f$-$3d$ spin-spin coupling is antiferromagnetic, leading to a parallel alignment of $3d$ and $4f$ moments in light rare-earth compounds and an antiparallel alignment in heavy rare earth compounds.[23–25] This universal picture can be understood by considering the role of hybridization between $5d$ and $3d$ states.[26] Within the framework of two-sublattice mean-field mode[27] and an assumption of a free ion moment for R, the moment of the G sublattice can be deduced from the total moment observed. Such an approach is particularly reasonable in the case of Gd compounds in which crystal-field ef-

fects can be neglected.[28] Assuming that Gd^{3+} moment takes its free ion value ($7\mu_B$) and is antiparallel to the global Fe moment, one can obtain the average moment of Fe, $\langle \mu_{Fe} \rangle$, over all Fe atoms at different crystallographic sites. The $\langle \mu_{Fe} \rangle$ characterizes a filling of d bands.[12] The dependence of the Curie temperature on the $\langle \mu_{Fe} \rangle^2$ is also plotted in Fig. 4.

Figure 4 shows that both T_C and M_S decrease with increasing Re concentration, following the usual trend of the effect of U substitution on the magnetic properties of $R(\text{Fe},U)_{12}$ compounds. In addition, according to the linear relationship between T_C and x ($x = 0.8-2.4$), $T_C = 553$ K was derived at $x = 0.694$, which is equal to the Curie temperature of the sample with $x = 0.6$, as shown in Fig. 4. This, in combination with the fact that the Curie temperature of the sample with $x = 2.6$ is almost identical to that for $x = 2.4$, indicates that the homogeneous regime of GdFe$_{12-x}$Re$_x$ is $x = 0.7-2.4$, consistent with the result derived from the composition dependence of lattice constants (Fig. 3).

The Curie temperature decreases at a rate of 102 K per Re atom, according to which the Curie temperature of the hypothetical GdFe$_{12}$ compound is derived to be 627 K, comparable to 600 K extrapolated from Gd(Fe,Al)$_{12}$ compounds.[29] Within the framework of the mean-field theory, there exist three kinds of exchange interactions in R-G (R=rare earth and G=transition metal) intermetallics, i.e. G-G, R-G and R-R interactions. At high temperature it is reasonable to neglect the much smaller R-R interaction relative to the G-G and R-G interactions. Thus, the Curie temperature of R-G intermetallics is determined predominantly by the G-G and R-G exchange interactions. The standard mean-field expression for the Curie temperature reads as[27]

$$3kT_{C,R} = a_{GG} + [a_{GG}^2 + 4a_{RG}a_{GR}]^{1/2} \quad (1)$$

where

$$a_{GG} = Z_{GG}J_{GG}S_G(S_G+1) \quad (2)$$

and

$$a_{RG}a_{GR} = Z_{RG}Z_{GR}S_G(S_G+1)(g_R-1)^2 J_R(J_R+1)J_{RG}^2. \quad (3)$$

The quantities Z_{GG}, Z_{RG} and Z_{GR} represent the number of G neighbors to the G atom, of G neighbors to the R atom and of R neighbors to the G atom, respectively. S_G is the quasispin of the G ions, defined by $\mu_G = 2S_G$. J_R is the total angular momentum quantum number of the rare earth R. J_{RG} can be derived from the following expression:

$$\left(\frac{J_{RG}}{k} \right)^2 = \frac{9T_{C,R}(T_{C,R}-T_{C,0})}{4Z_{RG}Z_{GR}S_G(S_G+1)(g_R-1)^2 J_R(J_R+1)}, \quad (4)$$

where $T_{C,0}$ represents the Curie temperature of compounds containing R=Y, La, Lu. Therefore, using $T_{C,0} = 460$ K for YFe$_{10.8}$Re$_{1.2}$ (Ref. 30) and $T_{C,R} = 506$ K for GdFe$_{10.8}$Re$_{1.2}$ in this work, one can estimate that $J_{\text{GdFe}} = -6.5$ K, close to $J_{\text{GdFe}} = -8.8$ K derived from the mean-field approximation for GdFe$_{10}$Mo$_2$ with $T_C = 430$ K.[12]
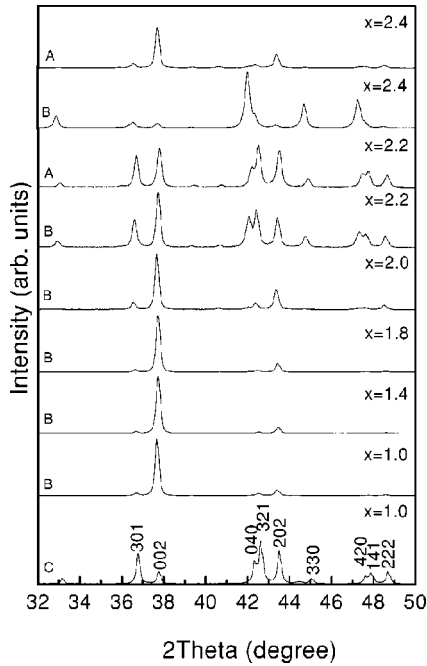
FIG. 5. XRD patterns of the magnetically aligned and unaligned samples of $GdFe_{12-x}Re_x$. (a) rotationally aligned, (b) normally aligned, (c) random powder.

FIG. 6. Field dependences of magnetization of $GdFe_{12-x}Re_x$ at 5 K.

Figure 4 reveals that for $GdFe_{12-x}Re_x$ the replacement of one Fe atom by Re gives rise to a reduction of $5.5\mu_B$/f.u. in M_S. For a comparison, included in Fig. 4 is also the case of the simple dilution model. The magnetic dilution model gives a reduction rate of $1.59\mu_B$/f.u. per Re atom, much smaller compared to the experimental value. This indicates that the reduced moment arising from the magnetic dilution by one Re atom could account for about 29% of the experimental reduction of the saturation moment. Band-structure calculations performed on $YFe_{12-x}Mo_x$ (Ref. 31) reveal that the occupation of one Mo atom over the $8i$ site leads to about $0.7\mu_B$ reduction of the total Fe moment due to the hybridization of the Fe $3d$ and Mo $5d$ bands. Therefore, magnetic dilution and hybridization effects account for about 50% of the reduction of the saturation moment. Although the number of $6s$ electrons of Re is one more than that of Mo, it is unreasonable to attribute the remaining 50% of the reduced saturation moment to this effect. So there must exist other causes responsible for the reduction of saturation moment, which will be discussed in Sec. IV.

2. Magnetocrystalline anisotropy

XRD experiments of the magnetically aligned samples were used to determine the EMD of $GdFe_{12-x}Re_x$ at room temperature. The magnetically aligned samples are categorized into two groups, denoted as the normally and rotationally aligned samples, respectively. The normally aligned sample was prepared by mixing fine-powder particles (≤ 20 μm) with epoxy resin at a weight ratio of 1:1, filling the mixture in a disklike container and placing it in an applied magnetic field of 1 T parallel to its axis at room temperature until the mixture solidified. The rotationally aligned
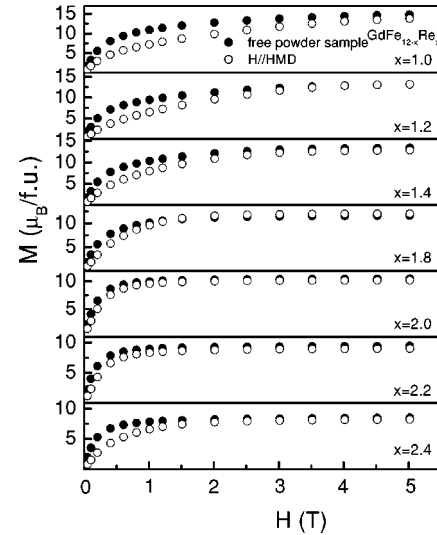
sample was made in a similar way, but the container was mounted on a rotating motor and placed in an applied magnetic field of 1 T perpendicular to its axis at room temperature until the mixture solidified. Included in Fig. 5 are the XRD patterns of the unaligned and magnetically aligned samples $x=1.0$–2.4) at room temperature. For the normally aligned samples with $x=1.0$–2.0, the (002) peaks are strongly intensified and other peaks are weakened or do not appear at all, which means the EMD along the c axis. Meanwhile, that the uniaxial anisotropy is gradually weakened by increasing Re content can be inferred from the decreasing ratio of peak intensity I_{002}/I_{202}, as indicated by Fig. 5. When $x=2.4$, the (040), (330), and (420) peaks for the normally aligned sample become very strong while the (002) peak is much intensified for the rotationally aligned sample, suggesting that the EMD is of easy plane. However, for the normally and rotationally aligned samples with the intermediate composition $x=2.2$, no specific peaks are intensified or weakened. The intensity ratio of I_{002}/I_{301} for the normally aligned sample is obviously greater than that for the rotationally aligned sample, while the intensity ratio I_{002}/I_{301} for the random-powder sample with $x=2.2$ (Fig. 1) is much smaller than those both for the normally and rotationally aligned samples. These observations reveal that the crystallographic orientation of powder particles did respond to the applied magnetic field upon being magnetically aligned and was different from a random distribution, indicating that the magnetocrystalline anisotropy of the compound with $x=2.2$ is not equal to zero but exhibits an EMD probably canted from the c axis. Hence, a change from uniaxial to probably canted to planar with increasing x occurred. The similar transition was also observed in $NdFe_{12-x}Mo_x$, $NdFe_{12-x}Mo_xN_{1-\delta}$ and $YFe_{12-x}Mo_xN_y$ (Refs. 19,20 and 32) as x increases.

The field dependences of magnetization of the free fine-powder and magnetically aligned samples of $GdFe_{12-x}Re_x$ at 5 K are given in Fig. 6. According to the aforementioned method in Sec. II, the anisotropy fields H_A of $GdFe_{12-x}Re_x$ for different x values were derived and given in Table II.
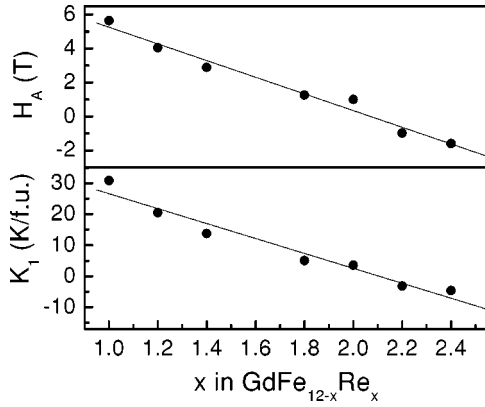
FIG. 7. Re content dependences of the magnetocrystalline anisotropy field H_A and the anisotropy constant K_1 of $GdFe_{12-x}Re_x$ at 5 K.

Here we denote the value of planar or canted anisotropy field as negative. Presented in Fig. 7 is the variation of H_A with x, which exhibits an almost-linear relationship between H_A and x. The substitution of Re for Fe leads to a tendency of weakening the uniaxial anisotropy of the $GdFe_{12-x}Re_x$ compounds, which is in good accord with the analyses of the XRD patterns shown in Fig. 5.

Since the Gd sublattice makes no contribution to the CEF-induced anisotropy of $GdFe_{12-x}Re_x$, the Fe sublattice favors the EMD parallel to the c axis and its magnetocrystalline anisotropy changes with increasing Re content. Phenomenologically, the anisotropy energy E_A may be expressed by[33]

$$E_A(\theta,\varphi) = K_1 \sin^2\theta + K_2 \sin^4\theta + K_3 \sin^4\theta \cos^4\varphi + \cdots, \tag{5}$$

where K_1, K_2, and K_3 are the anisotropy constants and θ and φ are the polar angles for the magnetization relative to the crystallographic axes. It has been established that the magnitude of the Fe sublattice anisotropy is dominated by the anisotropy constant K_1, compared with which much smaller K_2 can reasonably be neglected.[34] This allows us to evaluate the K_1 values of $GdFe_{12-x}Re_x$ in terms of the formulas $K_1 = M_S H_A/2$. The K_1 value at 5 K for $GdFe_{11}Re$ obtained in this way is about 30.8 K f.u.$^{-1}$, larger than the values 24.0 and 25.7 K f.u.$^{-1}$ for $YFe_{11}Ti$ (Ref. 34) and $YFe_{11.35}Nb_{0.65}$,[8] respectively. The variation of K_1 with Re concentration is shown in Fig. 7. From the Re concentration dependence of K_1, one can derive $x_{K_1,0} = 2.1$ for $K_1 = 0$.

For compounds with different crystallographic sites occupied by $3d$ metal, K_1 can be expressed as[35]

$$K_1 = \sum_{i=1}^{m} n_i K_1^i \tag{6}$$

where n_i is the number of sites i in the unit cell and K_1^i is the contribution of the site i to K_1; m is the number of unequivalent crystallographic sites occupied by $3d$ metal. For $GdFe_{12-x}Re_x$ the Re atoms occupy the $8i$ site preferentially, K_1 can be written as

$$K_1 = 4(K_1^i + K_1^j + K_1^f) - K_1^i x. \tag{7}$$

According to the approximate linear relationship between K_1 and x shown in Fig. 7 and assuming that K_1^i, K_1^j, and K_1^f do not vary with x, $K_1^i = 24.1$ K f.u.$^{-1}$ and $K_1^j + K_1^f = -11.4$ K f.u.$^{-1}$ were derived, in good agreement with the result $K_1^i > -K_1^j - K_1^f > 0$ obtained by Hu *et al.*[36]

IV. DISCUSSION

A. Structure stability and occupation of Re

For $R(Fe,U)_{12}$ compounds, previous investigations of structure were mainly concentrated on those stabilizing elements $U = $ Ti, V, Mo, and Nb, etc., having a positive mixing enthalpy with rare earth and a substantially larger atomic radius than Fe. Mixing enthalpy and atomic size both favor the $8i$ site preference of U.[12] The Si element has a negative mixing enthalpy with rare-earth elements, but it also has a smaller atomic radius than Fe. From enthalpy and atomic size considerations, Si is expected to prefer the $8j$ and $8f$ sites.[11] Therefore, these elements cannot afford to discriminate the respective role of mixing enthalpy and atomic size in stabilizing the 1:12 structure. Re is considered as a suitable choice to study this effect. According to Miedema model,[37] the solution enthalpies of Re in Gd and Fe in Gd are figured out to be -14 kJ mol^{-1} and -4 kJ mol^{-1}, respectively. Hence, from enthalpy considerations, one would expect that the Re atoms preferentially occupy the $8f$ and $8j$ sites that have two nearest-neighboring Gd atoms and thus have a larger contact area with Gd compared with the $8i$ site (see Table I). However, it is noteworthy that the radius of the Re atom, 1.38 Å, is substantially larger than that of the Fe atom, 1.27 Å. Of the three nonequivalent crystallographic sites in the 1:12 structure, the average distances of the $8i$ site to nearest neighboring Fe atoms in $GdFe_{12-x}Re_x$ are the largest, about 2.70 Å, as outlined in Table I. Thus, the $8i$ site has a much larger volume than the $8f$ and $8j$ sites and can accommodate the Re atoms. If the Re atoms occupy the $8f$ and $8j$ sites, large distortions will be produced, being energetically unfavorable. Therefore, the atomic size effect dominates over the enthalpy effect in stabilizing the 1:12 compounds by Re, similar to the case of Re in $Gd_3Fe_{28}Re$.[38]

Although the stabilizing effect of Re in 1:12 compounds is essentially due to the size effect as other transition metals, such as, $U = $ Ti, V, Mo, Nb, etc., regardless of the negative solution enthalpy of Re in R, the enthalpy effect does play a critical role in some cases. For instance, the Al atoms in $GdFe_{10}Al_2$ preferentially occupy the $8j$ site.[29] Since the solution enthalpy of Al in Gd is about -132 kJ mol^{-1} and the atomic radius of Al is 1.43 Å, much larger than that of Fe. The enthalpy consideration expects the Al atoms to prefer the $8j$ site, whereas the atomic size effect favors the $8i$ site preference. Therefore, to investigate the stabilizing effect and preferential occupancy of U in $R(Fe,U)_{12}$ compounds, one has to take into consideration the interplay of atomic size and enthalpy effects.

B. The Curie temperatures and saturation moments

Within the framework of the spin-fluctuation theory of Mohn and Wohlfarth[39] the Curie temperature is presented by

$T_c \propto M_0^2 \chi_0^{-1}$, where M_0 is the zero-temperature magnetic moment per Fe atom. The enhanced susceptibility χ_0 is given by

$$\chi_0^{-1} = \frac{1}{4\mu_B^2}\left(\frac{1}{N_\uparrow(\varepsilon_f)} + \frac{1}{N_\downarrow(\varepsilon_f)} - 2I\right), \qquad (8)$$

where $N_\uparrow(\varepsilon_f)$ and $N_\downarrow(\varepsilon_f)$ are the spin-up and spin-down states of density (DOS) at the Fermi level and I is the Stoner parameter. Generally, upon the substitution of U for Fe in $R(Fe,U)_{12}$, U will make a contribution to the DOS dominated by Fe $3d$ states near the Fermi level and the contribution increases with increasing U content, as demonstrated by the band-structure calculations on $Y(Fe,Mo)_{12}$.[31] The Stoner parameter I changes little across the $R(Fe,U)_{12}$ series. Figure 4 reveals an almost-linear relationship between T_C and $\langle\mu_{Fe}\rangle^2$, indicating that the χ_0 term has little effect on the Curie temperature. Hence the reduction of the Curie temperature of $Gd(Fe,Re)_{12}$ is determined primarily by the reduction of the average Fe moment. As pointed out previously, the reduction of saturation moment can be partly attributed to the magnetic dilution effect and the hybridization of the Fe and Re d bands. Based on the calculation of the noncollinear spin structure performed on $YFe_{12-x}Mo_x$ by Lorenz et al.,[40] the reduction of saturation moment is in a large part caused by the disorder in the directions of the local Fe moments.

C. Magnetocrystalline anisotropy

Within the framework of the mean-field theory the S-state ion Gd^{3+} in the $Gd(Fe,Re)_{12}$ compounds has no contribution to the CEF-induced magnetic anisotropy and the Gd^{3+} moment is considered to be antiparallel to the total Fe moment. However, since the Fe-Fe nearest-neighbor interatomic distance varies between about 2.38 and 2.93 Å and the Fe-Fe exchange interaction is a function of the distance following the Slater-Néel curve with a zero close to 2.45 Å,[41] the Fe-Fe ferromagnetic and antiferromagnetic couplings coexist in these compounds. According to the physical picture proposed by Lorenz et al.,[40] at relatively low Re content the antiferromagnetic coupling is quite weak and locally outbalanced by stronger ferromagnetic interactions, and as a result the collinear Fe intrasublattice ferromagnetic coupling occurs to result in the EMD along the c axis, as observed in $GdFe_{12-x}Re_x$ for $x=1.0$–2.0. As the amount of the substitution of Re for Fe located at the $8i$ site increases, the Fe moments tend to span out in a wide angle with respect to the

c axis, and the Fe moments on the $8j$ site perpendicular to the c axis could appear. This implies that the Fe ferromagnetic coupling is weakened or the antiferromagnetic interaction is enhanced with increasing Re content, namely, the uniaxial anisotropy decreases, as evidenced by the experimental observations. When $x=2.2$, the global magnetization may tilt away from the c axis and nonlinear spin structures are formed depending on the competition of ferromagnetic and antiferromagnetic exchange interactions. As soon as the antiferromagnetic interaction overwhelms the ferromagnetic coupling, the planar anisotropy occurs, corresponding to the case of $x=2.4$. Therefore, the occurrence of the change of the anisotropy from uniaxial to probably canted to planar arises from the substitutional disorder of Re for Fe on the $8i$ site. Our experiments give a strong support for the physical picture given by Lorenz et al.[40] However, detailed investigation of the thermomagnetic curves of $Gd(Fe,Re)_{12}$ revealed no evidence of spin-glass-like behavior, at variance with the results on $Y(Fe, Mo)_{12}$.[42]

V. SUMMARY

The $GdFe_{12-x}Re_x$ compounds with $x=0.7$–2.4 crystallize in the tetragonal $ThMn_{12}$ structure. The Rietveld refinement of the XRD data revealed that the Re atoms exclusively occupy the $8i$ site, which is essentially due to the atomic size effect, regardless of the negative solution enthalpy of Re in Gd. The lattice parameter a and the cell volume V increase with increasing Re content while c remains almost constant. Increasing Re content leads to a remarkable reduction of the Curie temperature and the saturation moment. The reduction of the Curie temperature is predominantly attributed to the decrease of the average Fe moment. The substitutional disorder of Re for Fe on the $8i$ site, together with the simple magnetic dilution and the hybridization of Re and Fe d states, is responsible for the reduction of the saturation magnetization. The increase of Re content gives rise to a change of the magnetocrystalline anisotropy from uniaxial to probably canted to planar, which results from the competition between the Fe ferromagnetic and antiferromagnetic exchange interactions originating from the variation of the nearest-neighbor distances between Fe atoms and the substitutional disorder of Re for Fe located at the $8i$ site.

ACKNOWLEDGMENTS

[1] D. B. Mooij and K. H. Buschow, J. Less-Common Met. **136**, 207 (1988).

[2] K. Ohashi, Y. Tawara, R. Osugi, and M. Shimao, J. Appl. Phys. **64**, 5714 (1988).

[3] S. F. Cheng, V. K. Sinha, Y. Xu, J. M. Elbicki, E. B. Boltich, W. E. Wallace, S. G. Sankar, and D. E. Laughlin, J. Magn. Magn. Mater. **75**, 330 (1988).

[4] K. H. J. Buschow, D. B. De Mooij, M. Brouha, H. H. A. Smit, and R. C. Thiel, IEEE Trans. Magn. **MAG-24**, 1611 (1988).

[5] M. Jurczyk, J. Less-Common Met. **166**, 335 (1990).

[6] O. Moze, L. Pareti, M. Solzi, and W. I. F. David, Solid State Commun. **66**, 465 (1988).

[7] R. B. Helmeholdt, J. J. M. Vleggaar, and K. H. J. Buschow, J. Less-Common Met. **138**, L11 (1988).

[8] B. P. Hu, K. Y. Wang, Y. Z. Wang, Z. X. Wang, Q. W. Yan, P. L. Zhang, and X. D. Sun, Phys. Rev. B **51**, 2905 (1995).

[9] O. Moze, L. Pareti, and K. H. J. Buschow, J. Phys.: Condens. Matter **7**, 9255 (1995).

[10] J. A. De Campos, L. P. Ferreira, M. Godinho, J. M. Gil, P. J. Mendes, N. A. De Campos, I. C. Ferreira, M. Bououdina, M. Bacmann, J. L. Soubeyroux, D. Fruchart, and A. Collomb, J. Phys.: Condens. Matter **10**, 4101 (1998).

[11] K. H. J. Buschow, J. Appl. Phys. **63**, 3130 (1988).

[12] H. S. Li and J. M. D. Coey, in *Handbook of Magnetic Materials*, edited by K. H. J. Buschow (North-Holland, Amsterdam, 1991), Vol. 6, p. 1.

[13] M. Solzi, L. Pareti, O. Moze, and W. I. F. David, J. Appl. Phys. **64**, 5084 (1988).

[14] K. H. J. Buschow, J. Magn. Magn. Mater. **100**, 79 (1991).

[15] C. J. M. Denissen, R. Coehoorn, and K. H. J. Buschow, J. Magn. Magn. Mater. **87**, 51 (1990).

[16] X. C. Kou, E. H. C. P. Sinnecker, R. Grössinger, G. Wiesinger, T. Zhao, J. P. Liu, and F. R. de Boer, J. Magn. Magn. Mater. **140-144**, 1025 (1995).

[17] Y. Z. Wang, B. P. Hu, L. Song, K. Y. Huang, and G. C. Liu, J. Phys.: Condens. Matter **6**, 7085 (1994).

[18] R. Verhoef, F. R. de Boer, and Z. D. Zhang, J. Magn. Magn. Mater. **75**, 319 (1988).

[19] Y. Z. Wang, B. P. Hu, X. L. Rao, and G. C. Liu, J. Appl. Phys. **75**, 6226 (1994).

[20] H. Sun, M. Akayama, and H. Fujii, Phys. Status Solidi A **140**, K107 (1993).

[21] H. M. Rietveld, Acta Crystallogr. **229**, 151 (1967).

[22] R. Y. Young, A. Sakthirel, T. S. Moss, and C. O. Paiva-Santos, J. Appl. Crystallogr. **28**, 366 (1995).

[23] I. A. Campell, J. Phys. F: Met. Phys. **2**, L47 (1972).

[24] K. H. J. Buschow, in *Ferromagnetic Materials*, edited by E. D. Wohlfarth (North-Holland, Amsterdam, 1980), Vol. 1, p. 297.

[25] J. J. M. Franse and R. J. Radwanski, in *Handbook of Magnetic Materials*, edited by K. H. J. Buschow (North-Holland, Amsterdam, 1993), Vol. 7, p. 307.

[26] M. S. S. Brooks and B. Johansson, in *Handbook of Magnetic Materials* (Ref. 25), Chap. 3.

[27] K. H. J. Buschow, Rep. Prog. Phys. **54**, 1123 (1991).

[28] K. H. J. Buschow, Rep. Prog. Phys. **40**, 1179 (1977).

[29] X. Z. Wang, B. Chevalier, T. Berlureau, and J. Etourneau, J. Less-Common Met. **138**, 235 (1988).

[30] M. Jurczyk, J. Magn. Magn. Mater. **89**, L5 (1990).

[31] I. A. Al-Omari, S. S. Jaswal. A. S. Fernando, and D. J. Sellmyer, Phys. Rev. B **50**, 12 665 (1994).

[32] Y. Z. Wang, B. P. Hu, X. L. Rao, G. C. Liu, L. Yin, W. Y. Lai, W. Gong, and G. C. Hadjipanayis, J. Appl. Phys. **73**, 6251 (1993).

[33] K. H. J. Buschow, in *Handbook of Magnetic Materials*, edited by E. P. Wohlfarth and K. H. J. Buschow (North-Holland, Amsterdam, 1988), Vol. 4, p. 1.

[34] C. Aadía, P. A. Algarabel, B. García, M. R. Ibarra, A. Del Moral, N. V. Kudrevatykh, and P. E. Markin, J. Phys.: Condens. Matter **10**, 349 (1998).

[35] N. P. Thuy, J. J. M. Franse, N. M. Hong, and T. D. Hien, J. Phys. C **8**, 499 (1988).

[36] B. P. Hu, H. S. Li, and J. M. D. Coey, J. Appl. Phys. **67**, 4838 (1990).

[37] A. R. Miedema, P. F. de Chatel, and F. R. de Boer, Physica B & C **100**, 1 (1980).

[38] W. G. Chu, G. H. Rao, H. F. Yang, G. Y. Liu, and J. K. Liang, J. Phys.: Condens. Matter **13**, L441 (2001).

[39] P. Mohn and E. P. Wohlfarth, J. Phys. F: Met. Phys. **17**, 2421 (1987).

[40] R. Lorenz, J. Hafner, S. S. Jaswal, and D. J. Sellmyer, Phys. Rev. Lett. **74**, 3688 (1995).

[41] L. Néel, Ann. Phys. (Paris) **5**, 232 (1936).

[42] C. Christides, A. Kostikas, G. Zouganelis, and V. Psyharis, Phys. Rev. B **47**, 11 220 (1993).